

Mechanisms of SWNT Probe-Sample Multistability in Tapping Mode AFM Imaging

Santiago D. Solares, Maria J. Esplandiu, William A. Goddard III,

and C. Patrick Collier

Supporting Information:

1. SWNT probe TEM image

Figure S-1 shows the TEM image of the SWNT probe used for the experimental measurements. As the picture shows, the probe has diameter and length of approximately 5.5 and 40 nm, respectively, and is tilted 15° with respect to the axis normal to the surface.

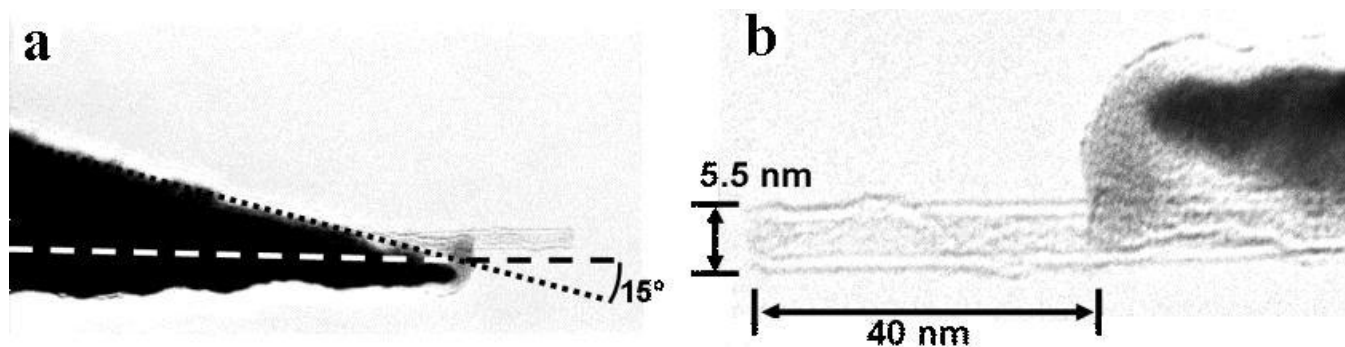


Figure S-1. TEM images of the SWNT probe used for the experimental measurements, mounted on a conventional silicon tip. The picture on the left (a) shows that the SWNT probe is tilted 15° with respect to

the axis normal to the substrate surface (dashed line). Picture (b) shows the SWNT probe dimensions. Reprinted from (*Nano Letters* **2004**, 4, 725-731). Copyright (2004) American Chemical Society.

2. Experimental procedure to image directly above the sample SWNT

To ensure that the experimental amplitude and force curves (Figure 5 of the paper) were acquired with the SWNT tip tapping directly on the crown of the sample SWNT, we performed the following procedure. Prior to conducting any measurements, we waited several minutes to minimize any drift. Then, under very low drift conditions, we reduced the scan size to have the sample SWNT in the middle and almost occupying the entire field of view. We again zoomed into the middle of the window (i.e. to the sample SWNT axis), reduced the scan size to zero and acquired the amplitude and phase curves. Finally we zoomed out back to the scan size corresponding to the width of the SWNT in order to verify that the sample was still at the same position (i.e. at the center of the scan window as before the measurement). We only kept and evaluated the measurements from cases in which the sample SWNT position did not change. In such cases, the acquired curves were reproducible.

3. Tip sample force curve of SWNT probe with silicon surface

Figure S-2 shows the tip-sample interaction force curve of the SWNT probe interacting with a bare silicon surface. This curve is similar to that of Figure 2 (b) of the paper, which corresponds to the same tip imaging a prone SWNT in sliding mode. The shifting of the force minimum is due to the presence of the sample, which requires that the probe bend around it before reaching the surface. The magnitude of the attractive force at the minimum is significantly smaller than for a conventional silicon tip (Figure 2 (a) of the paper).

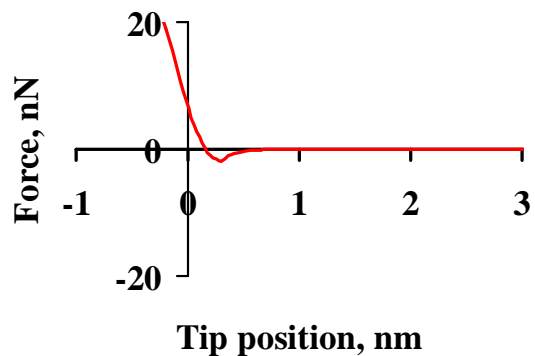


Figure S-2. Simulated tip-sample interaction force curve vs. tip position above the surface for the SWNT probe shown in Figure S-1 imaging a bare silicon surface.

4. Phase space representations

Figure S-3 shows the A_0 - Z_c “phase space” representation of the oscillation amplitude solutions for the SWNT tip *smooth gliding* mode and for a silicon tip, in the absence of tip-sample adhesion and friction forces. The initial tip velocity, V_0 , was set to zero. In both cases there are two distinct solutions to the amplitude, one corresponding to the attractive regime (phase $> 90^\circ$) and one corresponding to the repulsive regime (phase $< 90^\circ$). Qualitatively similar results were obtained for $V_0 = -0.0025$ nm/s and for $V_0 = 0.0025$ nm/s. This is consistent with the previous work of other authors.¹

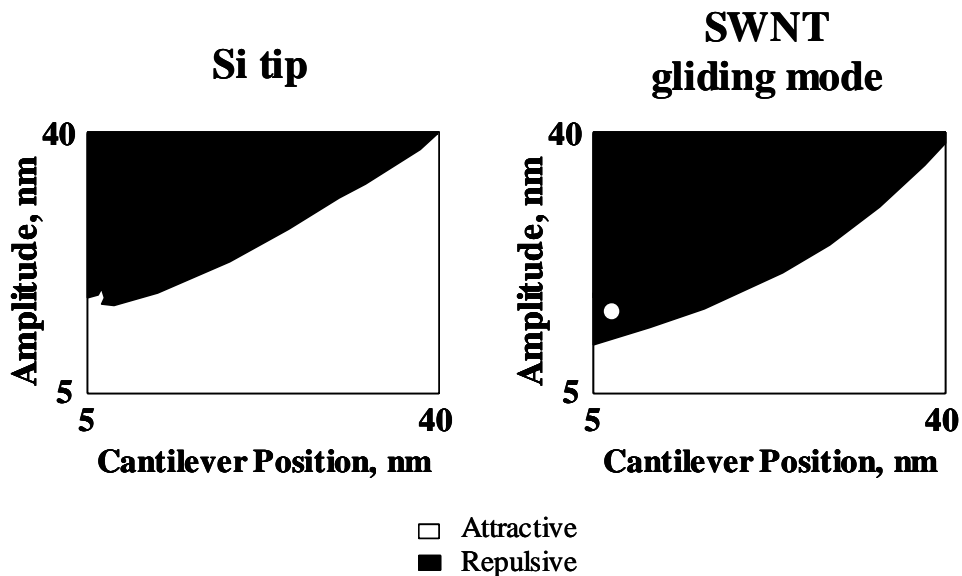


Figure S-3. A_0 - Z_c phase space representation of the two amplitude solutions for the conventional silicon tip and for the SWNT tip in *smooth gliding* mode for $V_0 = 0$, in the absence of tip-sample adhesion and friction forces.

5. Phase and amplitude curves (vs. cantilever position)

Figure S-4 shows the upper portion of the amplitude- and phase-position curves (vs. Z_c) for the SWNT smooth gliding mode and for the conventional silicon tip on the same coordinate system for $A_0 = 40$ nm and for $V_0 = 0$, in the absence of tip-sample adhesion and friction forces. These curves show typical behavior, in agreement with the diagrams of Figure S-3, with two amplitude solutions and a discontinuity between them.¹⁻² As the probe approaches the sample, the first solution occurs in the long-range attractive regime and the second solution occurs in the short-range repulsive regime. The amplitude in the attractive regime is lower than the amplitude in the repulsive regime for a given value of Z_c and F_0 (excitation force). The amplitude for the SWNT tip is larger than that of the conventional silicon tip for a given value of Z_c and F_0 , indicating greater probe penetration (as confirmed through MD simulations).

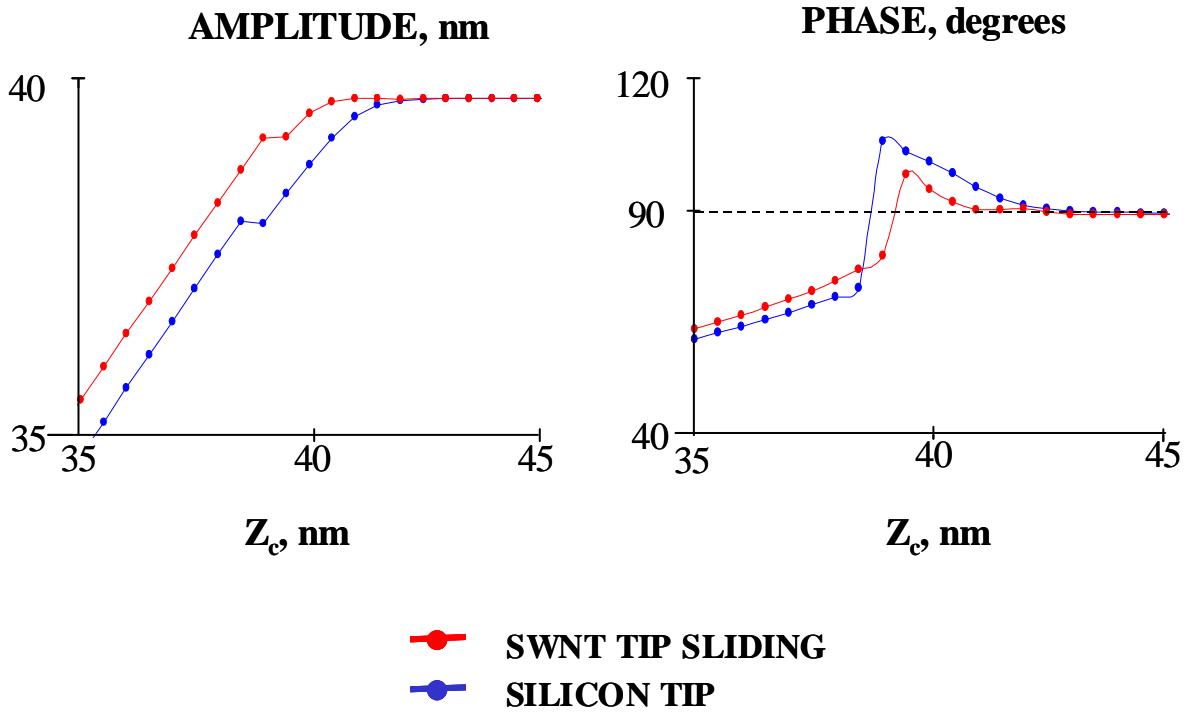


Figure S-4. Oscillation amplitude and phase vs. cantilever position for the Si tip (blue curves) and for the SWNT tip in *smooth gliding* mode (red curves), for $A_0 = 40$ nm and $V_0 = 0$ in the absence of tip-sample adhesion and friction forces.

Figure S-5 shows a tip-sample interaction force curve, the amplitude curve and the phase curve for the snapping case of Figure 2 (c) of the paper with the inclusion of a 25 nN tip-sample adhesion force at the points of initial tip-*sample* and tip-*surface* contact. The two attractive solutions (a snapped and an unsnapped oscillation) and one repulsive solution (snapped oscillation) are clearly discernible from both the amplitude and the phase curves. The other repulsive solution (unsnapped oscillation) does not occur due to the large adhesion force (attractive), which dominates the repulsive interactions in the region where snapping does *not* occur. The tip-sample interaction force curve illustrates the different behavior of the force in the upward and downward trajectories of the tip due to snapping, which takes place only during the *downward* motion of the probe, and due to the adhesion force, which acts only during the *upward* motion of the probe (the parameters and explicit functional forms used to model adhesion forces are given in tables S-1 and S-2).

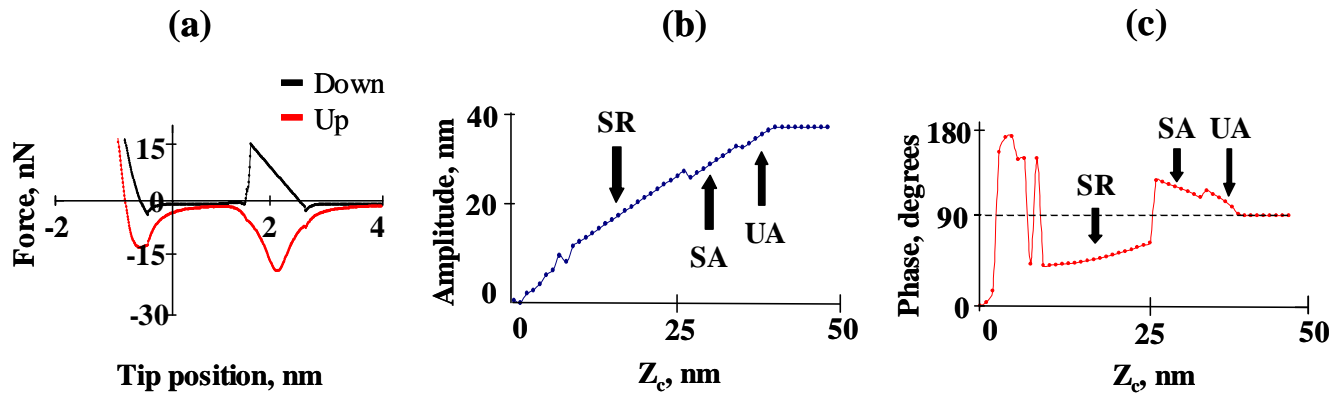


Figure S-5. Tip-sample force (a), amplitude (b) and phase (c) curves for the snapping case of Figure 2 (c) of the paper, with the inclusion of an adhesion force at the point where tip-sample contact first occurs and at the point where tip-substrate contact first occurs. Three solutions of the amplitude are discernible in the amplitude and phase curves: the snapped and unsnaped attractive solutions (SA and UA), and the snapped repulsive solution (SR). Note that the abscissa corresponds to the instantaneous tip position (z_{ts}) in curve (a), and to the cantilever rest position (Z_c) in curves (b) and (c). $A_0 = 40$ nm for curves (b) and (c).

6. Adhesion and friction force parameters and functional forms

Table S-1 provides the magnitude of the adhesion forces and contact quality factors used to construct the results presented in Figure 6 of the paper. Different values were used depending on the magnitude of the free oscillation amplitude and on whether or not the probe was able to snap during the oscillation. Table S-2 contains the functional forms used to simulate the adhesion forces. z_{ts} represents the distance from the tip to the substrate surface. The value of z_{ts} for which tip-sample contact first occurs is 2.54 nm in all cases. In all cases, the *magnitude* of the adhesion force has a maximum at a tip position slightly lower than the point of initial tip-sample contact, and decreases in both directions, as illustrated in Figure S-5 (a). These functional forms, determined through trial and error, were the ones that allowed us to most closely reproduce the experimental results.

Table S-1: Magnitude of the contact quality factor and of the maximum adhesion force for the simulation results of Figure 6.*

	Figure 6 (a)	Figure 6 (b)	Figure 6 (c)
Contact quality factor, <i>unsnapped</i> oscillations	0.005	0.008	0.005
Contact quality factor, <i>snapped</i> oscillations	N/A	N/A	0.0045
Maximum adhesion force, <i>unsnapped</i> oscillations, nN	21.5	21.5	20
Maximum adhesion force, <i>snapped</i> oscillations, nN	N/A	N/A	5

*Note that snapping did not occur for the results shown in Figures 6 (a) and 6 (b), so no parameters are provided for *snapped* oscillations for those cases.

Table S-2: Functional forms used to simulate the adhesion forces (F_a) in the construction of the phase and amplitude curves shown in Figure 6 of the paper (z_{ts} is the tip-surface distance in nm).*

Simulation	Functional form of the adhesion force
Figure 6 (a)	$F_a = \frac{-21.5}{1 + 2.5(z_{ts} - 1.86)^{2.75}}, \text{ for } z_{ts} > 1.86$ $F_a = 1000 z_{ts} - 1.86 ^3 - 21.5, \text{ for } z_{ts} < 1.86 \text{ and } z_{ts} > 1.58$
Figure 6 (b)	$F_a = \frac{-21.5}{1 + 2.5(z_{ts} - 1.86)^{2.75}}, \text{ for } z_{ts} > 1.86$ $F_a = 1000 z_{ts} - 1.86 ^3 - 21.5, \text{ for } z_{ts} < 1.86 \text{ and } z_{ts} > 1.58$
Figure 6 (c), <i>unsnapped</i> oscillations	$F_a = \frac{-20}{1 + 2(z_{ts} - 2)^2}, \text{ for } z_{ts} > 2$

oscillations

$$F_a = \frac{-20}{1 + 275(z_{ts} - 2)^4}, \text{ for } z_{ts} < 2 \text{ and } z_{ts} > 1.5$$

Figure 6 (c), *snapped*

$$F_a = \frac{-5}{1 + 75(z_{ts} - 2)^2} \text{ for } z_{ts} > 2$$

oscillations

$$F_a = \frac{-5}{1 + 275(z_{ts} - 2)^4} \text{ for } z_{ts} < 2 \text{ and } z_{ts} > 1.5$$

*Recall that the adhesion force acts only during the upward motion of the probe *after it has contacted the sample*. Different functions were used for snapped and unsnapped oscillations in the construction of Figure 6 (c).

7. Simulation results for other sample geometries

Si(111)-CH₃ step edges:

Figure S-6 contains the energy⁴ and force curves for a 30,30 SWNT probe (4.1 nm diameter) approaching the step edge of a Si(111)-CH₃ surface (Figure S-7). The results indicate that snapping can occur for this type of geometry and dimensions. The labels on the curves of figure S-6 correspond to the MD snapshots of figure S-7 and show the behavior of the probe as it approaches the sample. The phase and amplitude curves are shown in figure S-8, $A_0 = 20$ nm. Both the amplitude and the phase curves exhibit multistability, similar to the curves of figure 4 of the paper.

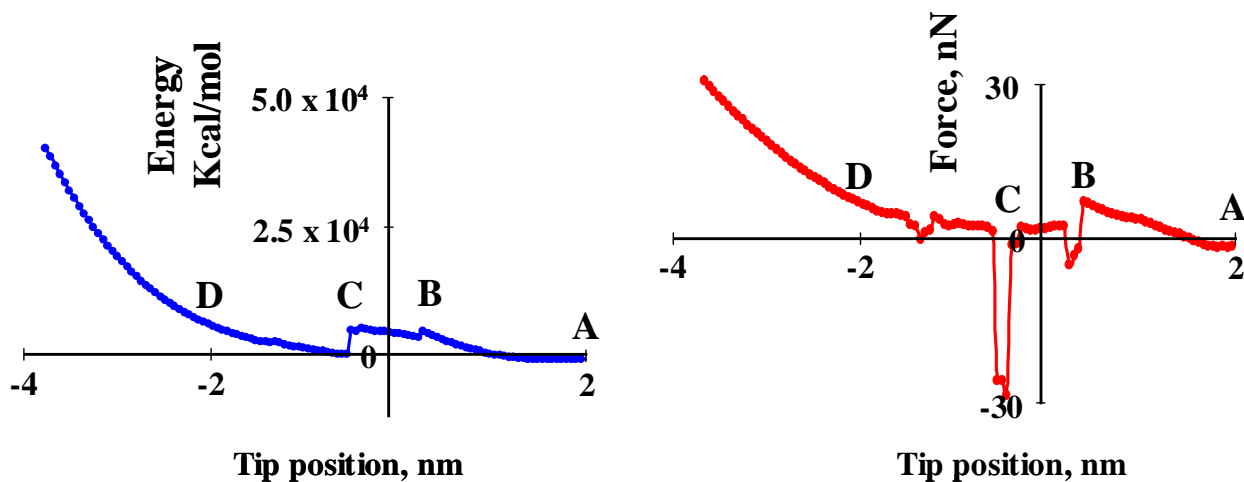


Figure S-6. Energy and force vs. tip position for a 30,30 SWNT tip approaching the step edge of a Si(111)-CH₃ surface. The labels A, B, C and D correspond to the MD snapshots of Figure S-7.

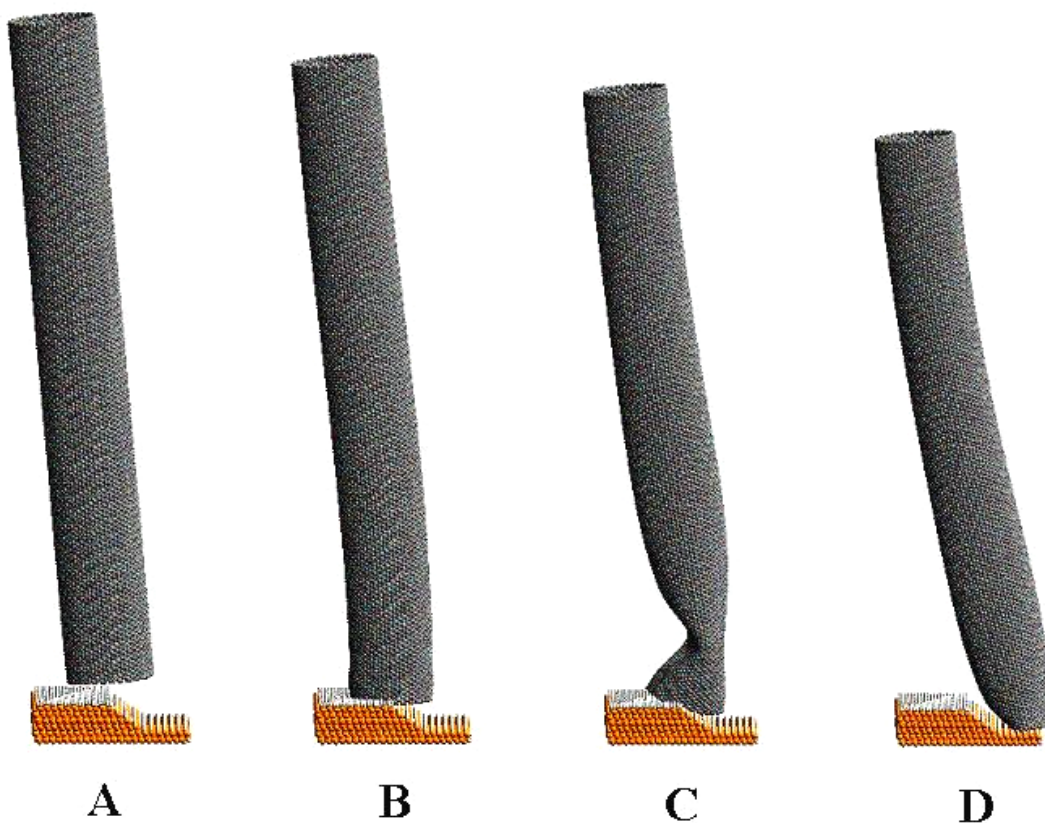


Figure S-7. MD snapshots of a 30,30 SWNT approaching the step edge of a Si(111)-CH₃ surface illustrating the snapping mechanism for this geometry. The labels correspond to those shown on the energy and force curves of figure S-6.

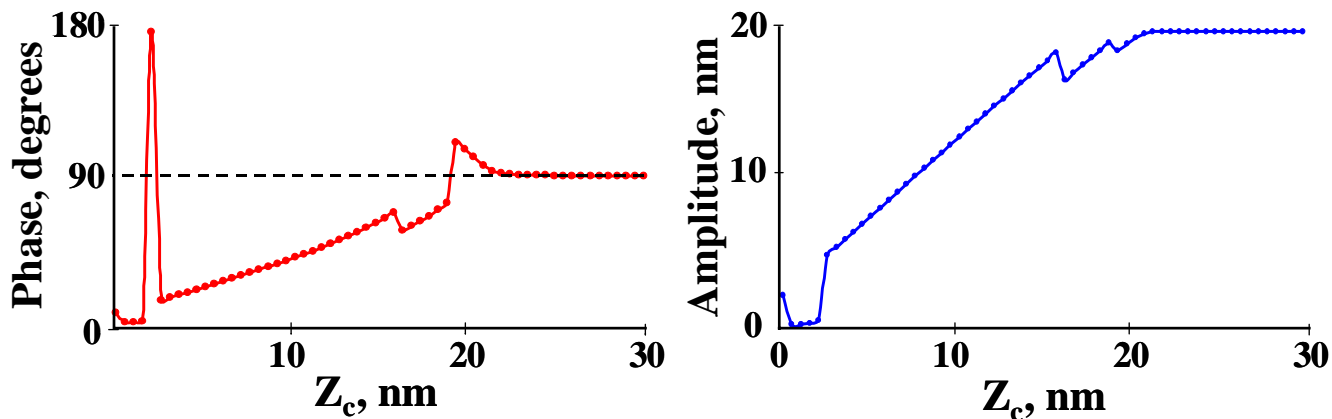


Figure S-8. Phase and amplitude curves constructed using the force curve of Figure S-6. Three amplitude solutions are clearly discernible in both curves ($A_o = 20$ nm).

4.7 nm Au nanoparticles:

Figure S-9, S-10 and S-11 show the results for the simulation of a 30,30 SWNT probe (4.1 nm diameter) imaging a 4.7 nm Au nanoparticle, in the absence of adhesion and friction forces. These results confirm that snapping can also occur for this system. The amplitude curve shows well defined regions corresponding to the type of oscillation that took place (figure S-11): region A is the free oscillating amplitude, regions B and E correspond to the range of cantilever positions for which the probe did not snap off the Au nanoparticle, region C corresponds to the range of cantilever positions for which the probe snapped off the Au nanoparticle every oscillation but did not reach the surface, and region D corresponds to the range of cantilever positions for which the probe snapped off the Au nanoparticle and reached the surface during every oscillation. The phase curve clearly shows the transitions between the different attractive and repulsive solutions.

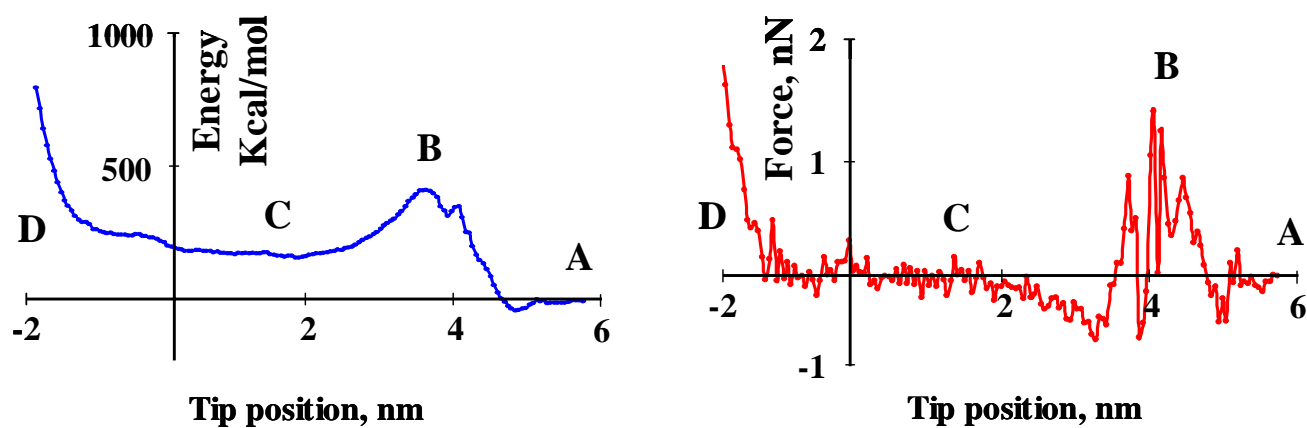


Figure S-9. Energy and force Vs. tip position for a 30,30 SWNT tip imaging a 4.7 nm Au nanoparticle.

The labels A, B, C and D correspond to the MD snapshots of Figure S-10.

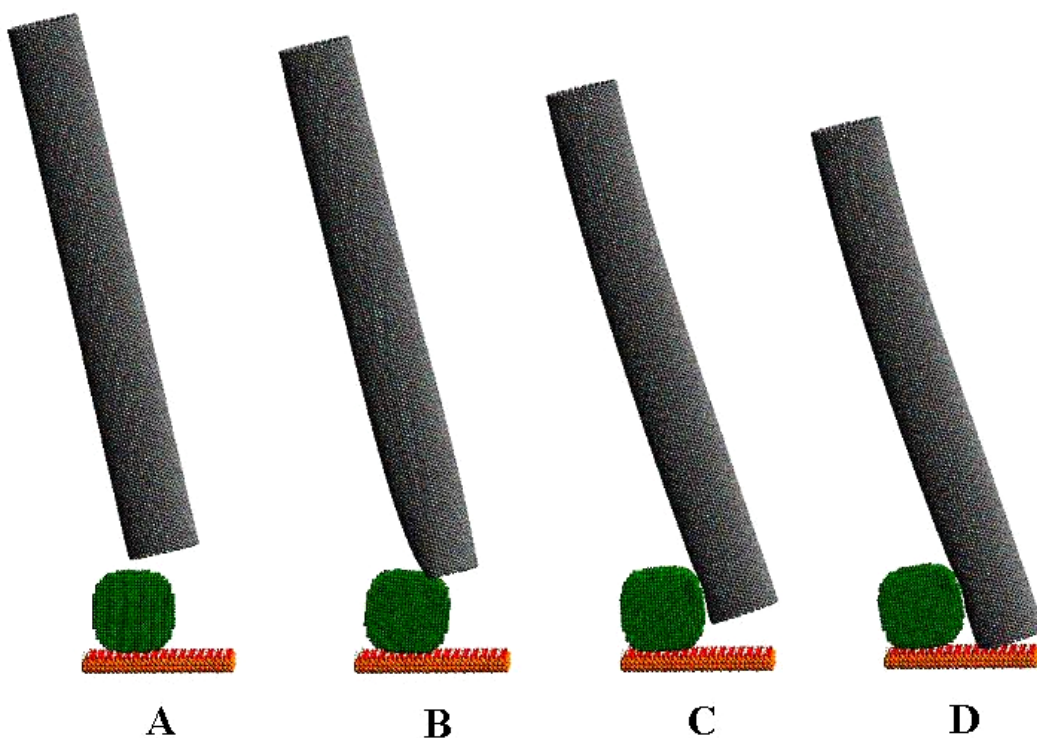


Figure S-10. MD snapshots of a 30,30 SWNT approaching a 4.7 nm Au nanoparticle, indicating that snapping can also occur for this system. The labels correspond to those shown on the energy and force curves of figure S-9.

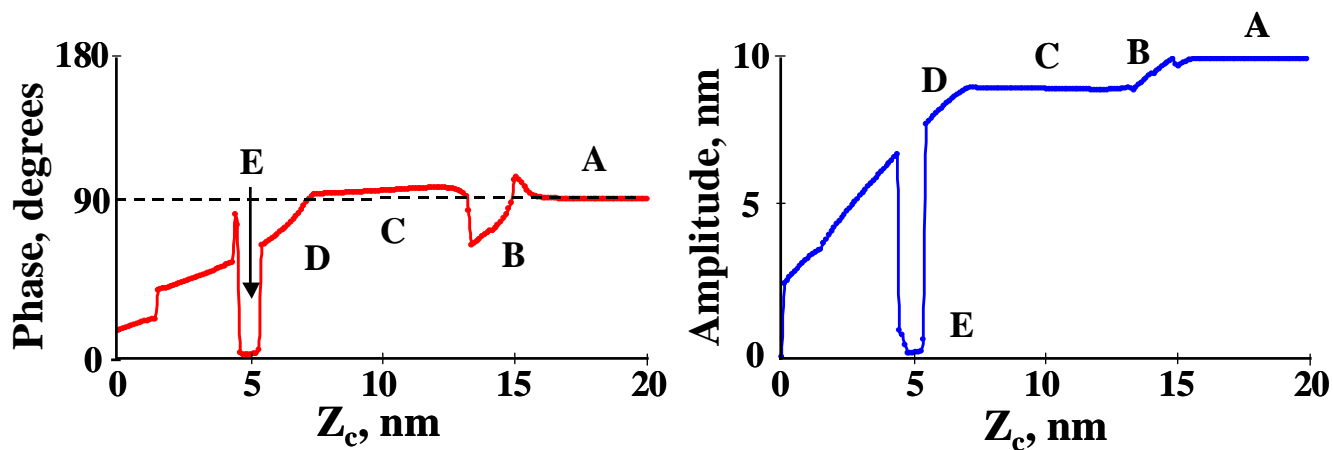


Figure S-11. Phase and amplitude curves constructed using the force curve of Figure S-9. Multiple regimes are clearly discernible in both curves: free oscillation (A), unsprung oscillations (B and E), sprung oscillations without reaching the substrate surface (C), and sprung oscillations reaching the surface (D). $A_0 = 10$ nm.

8. Additional MD parameters

We have provided the MD parameters for SWNT's and Si systems in our previous publication.⁴ The additional parameters, required for the simulation of the Si(111)-CH₃ surface step edge and for the Au nanoparticle, were taken from the Dreiding Force Field³ (with the H-C-Si-Si torsion barrier adjusted to 2.945 kcal/mol based on ab initio QM calculations on the Si(111)-CH₃ surface) and from the work of Jang et al.⁵ on Au surfaces (using a 6-12 Lennard-Jones function for the Au – C interaction, with $R_0 = 4.5$ Angstroms, and $D_0 = 0.175$ kcal/mol).

9. References

1. García, R.; Perez, R. *Surf. Sci. Reports* **2002**, *47*, 197.
2. García, R.; San Paulo, A. *Phys. Rev. B* **1999**, *60*, 4961.
3. Mayo, S. L.; Olafson, B. D.; Goddard, W. A. *J. Phys. Chem.* **1990**, *94*, 8897.

4. Shapiro, I.R.; Solares, S.D.; Esplandiu, M.J.; Wade, L.A.; Goddard, W.A.; Collier, C.P. *J. Phys. Chem. B* **2004**, *108*, 13613.

5. Jang, S.S.; Jang, Y.H.; Kim, Y-H.; Goddard, W.A.; Flood, A.H.; Laursen, B.W.; Tseng, H-R.; Stoddart, J.F.; Jeppesen, J.O.; Choi, J.W.; Steuerma, D.W.; DeIonno, E.; Heath, J.R.; *J. Am. Chem. Soc.* **2005**, *127*, 1563.